Phys. Status Solidi C **6**, No. 3, 707–715 (2009) / **DOI** 10.1002/pssc.200880713

physica status solidi c
www.pss-c.com
current topics in solid state physics

Silicon based IR light emitters

Martin Kittler[*, 1, 2], Teimuraz Mchedlidze[2], Tzanimir Arguirov[1, 2], Winfried Seifert[1, 2], Manfred Reiche[3], and Thomas Wilhelm[3]

[1] IHP, Im Technologiepark 25, 15236 Frankfurt (Oder), Germany
[2] Joint Lab IHP/BTU Cottbus, Konrad-Wachsmann-Allee 1, 03046 Cottbus, Germany
[3] Max-Planck-Institut für Mikrostrukturphysik, Weinberg 2, 06120 Halle, Germany

Received 10 June 2008, revised 12 September 2008, accepted 15 September 2008
Published online 14 January 2009

PACS 71.55.Cn, 71.70.Ej, 78.20.Jq, 78.55.Ap, 78.60.Fi, 85.60.Jb

[*] Corresponding author: e-mail kittler@ihp-microelectronics.com, Fax: +49 (0)335 5625 333, www.jointlab.de

A new concept for Si-based light emitting diodes (LED) capable of emitting at 1.5 µm is proposed. It utilizes D-band radiation from dislocations in Si. Whether a dislocation network created in a reproducible manner by Si wafer direct bonding or dislocation loops produced by Si ion implantation are employed. It is also stated that dislocation loops do not lead to the strong band-to-band electroluminescence at 1.1 µm of p-n diodes, as it was predicted in the literature. A MOS-LED (Fig. A) and p-n LEDs emitting at 1.5 µm are demonstrated by the authors. The maximum efficiency that could be achieved at room temperature is close to 1%. Levels in the bandgap which are probably involved in the formation of the D1-line at 1.5 µm are revealed. Moreover, the observation of the Stark effect for the D1-line is reported. Namely, a red/blue-shift of peak position was observed in electro- and photo-luminescence when the electric field in the p-n LED was increased/lowered. This effect may allow realization of a novel Si-based light emitter with electric field modulated emission wavelength.

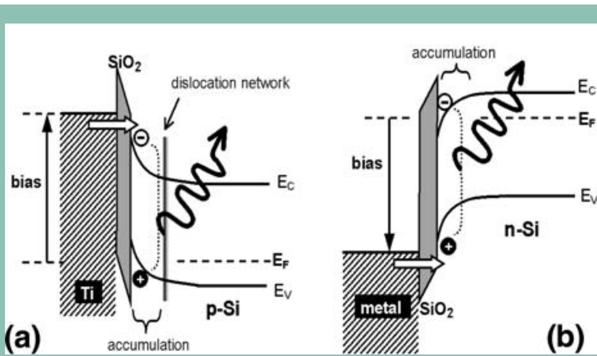

Scheme of MOS-LED, (a) p-type material with dislocation network, capable of yielding both dislocation and BB luminescence, (b) n-type Si without network yielding BB luminescence only.

1 Introduction Currently used interconnects based on Cu wiring will cause serious problems in the future such as heat penalty, non-acceptable delay and complexity, crosstalk etc. On- chip optical interconnects are able to overcome these problems and will be essential for future integrated circuits. Several CMOS-technology compatible key components have already been demonstrated. However, silicon based light emitter, which is compatible with CMOS technology, is still lacking. The recently demonstrated first Si-based Raman laser cannot be used for this purpose because it is optically pumped [1]. Different approaches for light emitters have been studied [2]. Recently, light-emitting diodes (LED) made either by boron [3-7] or by phosphorus [7] implantation into Si attract special interest, allowing efficient room temperature (RT) electro-luminescence (EL) of the Si band-to-band (BB) line at 1.1 µm. However, the desired light emitter, besides exhibiting high luminescence efficiency at RT, should also be spatially confined and should emit at about 1.5 µm. The D1 emission close to 1.5 µm, related to dislocations in Si, is a suitable candidate for the light emitter [8], but application of dislocations as active device components requires their reproducible formation.

We have demonstrated a MOS-LED [9] and a p-n LED emitting at 1.5 µm (D1 line) which are based on a dislocation network formed during direct bonding of Si wafers [10]. In another publication [11] we reported on electroluminescence (EL) around 1.5 µm from dislocation loops formed after Si ion implantation and annealing. The application of various Si-based light emitters presented so far and including those described in [1, 3, 12] requires a separate electro-optical devices for modulation of the emission. Fast modulators that can be integrated on a chip have been demonstrated already. The Mach-Zehnder modulator described by Liu et al. [13] occupies a large area on the chip. Another type of modulator based on the Stark effect in SiGe/Ge multiple quantum wells on Si was proposed by Kuo et al. [14]. The Stark effect on dislocation loops formed within the depletion layer of a p-n junction, reported in the present paper, allows a significant shift of the spectral position of the D1 peak by the bias-induced variation of the electric field in the junction. This effect may allow realization of a novel Si-modulator with the advantage of combining a dislocation-based light emitter and modulator within the same device. In the following, at first we will shortly present our LEDs emitting the dislocation-related D1-peak at 1.5 µm. Then the results related to the Stark effect will be presented and discussed.

2 LEDs exhibiting band-band radiation Light sources made by ion implantation are reported for example in [3-7]. The achievement of intense RT BB radiation after boron implantation and annealing has been attributed to the formation of dislocation loops which introduce a local strain field modifying the Si band structure locally, thus preventing non-radiative recombination [3]. Furthermore, it was stated that engineering of {113} defects formed during the post anneal of the boron implant are the reason for an even stronger BB emission [6]. Despite the observation of strong BB radiation in conjunction with defects/dislocations its straight ascription to defects, as stated in [3, 6], is misleading.

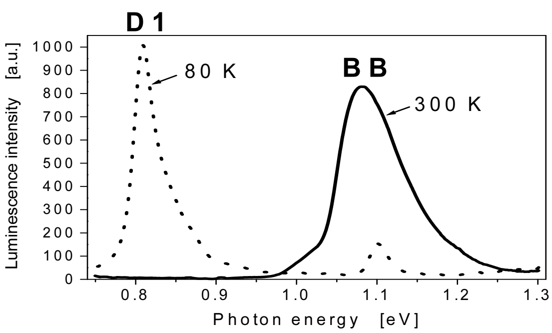

Figure 1 Defect and band-to-band emission in a Si diode fabricated by ion implantation: Photoluminescence spectra at 80 and 300 K, exhibiting BB and D1 line at 1.1 µm and 1.5 µm, respectively.

As seen from Figs. 1 and 2, the crystal defects do not emit the BB line but give rise to an additional spectral feature, namely the D1 line. Moreover, BB emission arises mainly from the defect-free region. Figure 3 shows that the EL efficiency of the BB line in the LED increases with temperature T (anomalous behavior). For comparison, the regular temperature behavior of luminescence in as-grown Si is shown in the inset. Our model suggests a different explanation of the results [7]. It takes into account the three recombination components in Si, namely Shockley-Read-Hall (SRH) recombination via deep levels in the band-gap, Auger recombination with energy transfer to a third carrier and the radiative BB recombination [15].

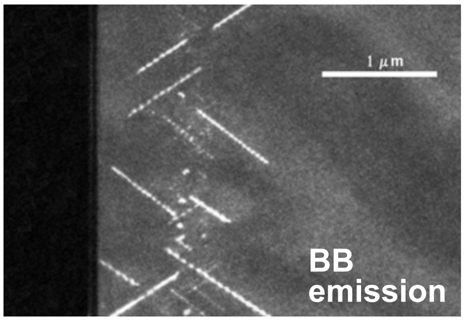

Figure 2 Example of crystal defects formed after ion implantation and subsequent annealing: Cross-sectional TEM image (dark field) of a sample after P implantation (750 keV, 2×10^{14} cm^{-2}) and furnace anneal (1000 °C, 30 min). The region where mainly BB line arises is also indicated.

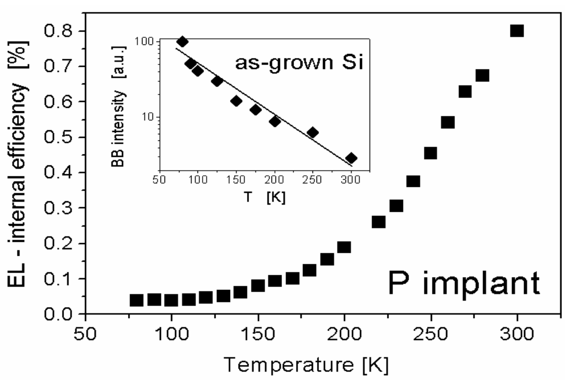

Figure 3 Efficiency of electro-luminescence: Anomalous T behavior of the BB line (1.1 µm) of EL observed at 1.2 V forward bias in a diode formed by P implantation into p-Si (10 Ωcm); implantation at 500 keV, $4\text{x}10^{14}$ cm^{-2} followed by furnace anneal (1000 °C, 30 min). The inset represents the regular T behavior of luminescence in as-grown Si.

The recombination rates R of these three mechanisms depend on the excess carrier concentration Δn. For the SRH recombination the rate is given by $R_{SRH} = \Delta n \cdot 1/\tau_{SRH}$, where τ_{SRH} denotes the SRH lifetime. The dependence of the radiative recombination rate and the Auger recombination rate on Δn are given by $R_{BB} \sim \Delta n^2 \cdot B$ or $R_{Auger} \sim \Delta n^3 \cdot C$, respectively. Here, B denotes the radiative recombination coefficient (for BB recombination) and C is the Auger recombination coefficient. The internal quantum efficiency is defined by the ratio of the radiative recombination rate R_{BB} and the overall recombination rate, i.e. $\eta_i = R_{BB}/(R_{SRH} + R_{BB} + R_{Auger})$. Figure 4 depicts the calculated internal quantum efficiency η_i as a function of the excess charge carrier density Δn, e.g. the carriers formed close to a forward biased p-n junction. The calculation was done for 300 K by using following values for the coefficients: $B = 10^{-14}$ cm^3s^{-1} [16] and $C = 10^{-31}$ cm^6s^{-1} [17], with the SRH lifetime τ_{SRH} as a parameter. Note that $1/\tau_{SRH}$ is proportional to the concentration N_T of traps/impurities characterizing the quality of the bulk material. Also the coefficients B and C reflect bulk properties. Hence, the model postulates that the intensive EL of the BB line escapes from the Si bulk (below the p-n junction) and is not formed at/around crystal defects as stated in [3, 6]. The efficiency for light emission is largely governed by the SRH lifetime. The implantation-related crystal defects may improve τ_{SRH} in the bulk due to their gettering action, i.e. they support reaching a strong BB emission in an indirect way. In nearly perfect Si bulk material with $\tau_{SRH} = 10^{-3}$ s the maximum of the quantum efficiency η_i is expected to reach about 30% at 300 K. This value is in agreement with that of Trupke et al. who concluded from their experimental data that the internal quantum efficiency of Si at 300 K might exceed 20% [18].

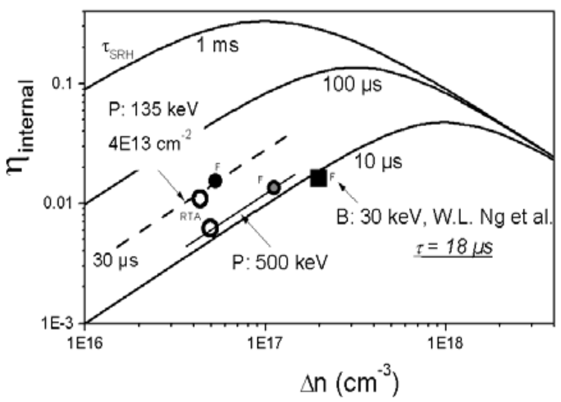

Figure 4 Internal quantum efficiency vs. excess carrier concentration calculated with SRH lifetime as parameter. Experimental data points for diodes implanted with P at energies of 135 and 500 keV, respectively, are shown together with data for B implantation from Ng et al. [3].

Figure 4 demonstrates the agreement of our experimental data (circles) with the model. The efficiency values η have been measured and the corresponding values of the excess carrier density Δn have been calculated with the process and device simulator 'ISE TCAD' for the process conditions applied to fabricate the diodes and for the applied forward bias of 1.2 V. There is also a good correspondence of the model with experimental data published by Ng. et al. in [3]. The lifetime τ_{SRH} = 10 µs deduced by the model for the sample used in [3] (black square) is in a fairly good agreement with the measured lifetime of τ_{SRH} = 18 µs reported in [3]. The model allows explaining the anomalous T-behavior of the BB line as well, which is another argument for its validity [7]. Summarizing, this "bulk model" claims that the BB radiation is not spatially confined at/around the implantation related defects, but is generated in the interior of the Si bulk below the p-n junction. This model was verified experimentally too. Both, missing confinement of the BB radiation and its wavelength of about 1.1 µm are against the applicability of a Si LED made by ion implantation as on-chip light emitter. In contrast, a light emitter based on dislocation-related luminescence is a promising candidate for this task.

3 LEDs based on dislocation radiation

3.1 Dislocation-related luminescence in Si A typical dislocation-related luminescence (DRL) spectrum for dislocated Si with the quartet of defect-related D1-D4 peaks [19] is shown in the inset of Fig. 5. The D1 and D3 peaks appear at about 1.5 or 1.3 µm, respectively, i.e. at the wavelengths corresponding to the low absorption in fibber glass. For application of dislocations as active parts of LEDs their formation must be reproducible regarding both structure and location. Si wafer direct bonding using hydrophobic surfaces is a promising technique allowing formation of a regular dislocation network. Details of the bonding procedure were described in [20].

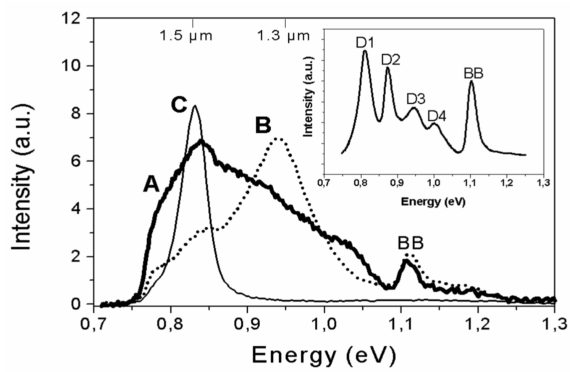

Figure 5 Example of an impact of misorientation / structure on the luminescence spectra of dislocation networks. (A) Twist angle of $\alpha = 9°$, dominating D1 peak; (B) Twist angle of $\alpha = 8.2°$, dominating D3 peak. Same tilt angle of $\beta = 0.2°$ in both cases. (C) Appearance of D1 line for the network shown in Fig. 6. The inset shows a typical spectrum of dislocated Si, exhibiting the D1-D4 DRL peaks and the BB peak.

An example TEM micrograph of a periodic dislocation network consisting of closely spaced screw and edge dislocations is represented in Fig. 6. The structure of a dislocation network, i.e., density and type of the dislocations formed, depends on the misorientation angles α and β for twist and tilt during wafer bonding. The dislocation network can be well reproduced by appropriate adjustment of the angles. The DRL spectra strongly correlate with the structure of the dislocation network (see Fig. 5). Hence, the DRL spectrum can be tailored by the misorientation angles in a controlled manner and dominance of either D1 or D3 radiation can be attained. A layer transfer treatment allows positioning the dislocation network close to the wafer surface, e.g. [21]. The network can be formed at depths ranging from less than 50 nm (see below, Fig. 11) to micrometers below the surface.

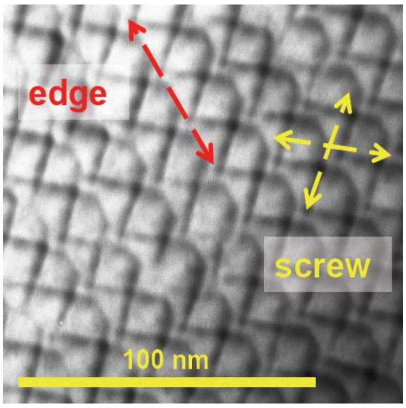

Figure 6 TEM plan view of a periodic dislocation network fabricated by direct bonding of (100) Si wafers. The directions of screw and edge dislocations are indicated. Note, for this network only the D1-peak was detected (see spectrum C in Fig. 5).

3.2 D1-line related energy levels in Si the bandgap It is well accepted that D4 is formed due to the transition between the 1-dimensional energy bands caused by the elastic strain field around the dislocation and that D3 is a phonon replica of D4. However, the energy levels that form the D1 and D2 lines are still under discussion. Recent models [22, 23] suppose that the D1 line is a result of carrier transition between two, relatively deep and relatively shallow energy levels in Si bandgap. If this model is true, the temperature dependence of the EL intensity - EL(T) - should exhibit two activation energies relevant to the energy levels. Moreover, the dependence of the EL intensity on the carrier injection level EL(J) - which saturates for certain injection level - is also affected by the temperature T. This is caused by the influence of T on the level population. Therefore, investigation of the EL(T) dependence could be done only by analyzing the change of the EL(J) dependencies with temperature. Results of such investigation are presented in Fig. 7a. Each maximum of the EL(J) curves - appearing at a certain J value - corresponds to a condition where the thermal excitation from the dislocation states is equalized by the injected carriers. Thus, Arrhenius plots for these certain J values could give information about the position of the dislocation related levels in the bandgap. The obtained results suggest two shallow levels, i.e. $E_1 = 0.09$ eV and $E_2 = 0.29$ eV (see Fig. 7b). These levels correspond well to dislocation-related DLTS peaks. Moreover, the value of the sum $E_1 + E_2 + E_{D1}$ is close to the energy of Si bandgap (see inset in Fig. 7b).

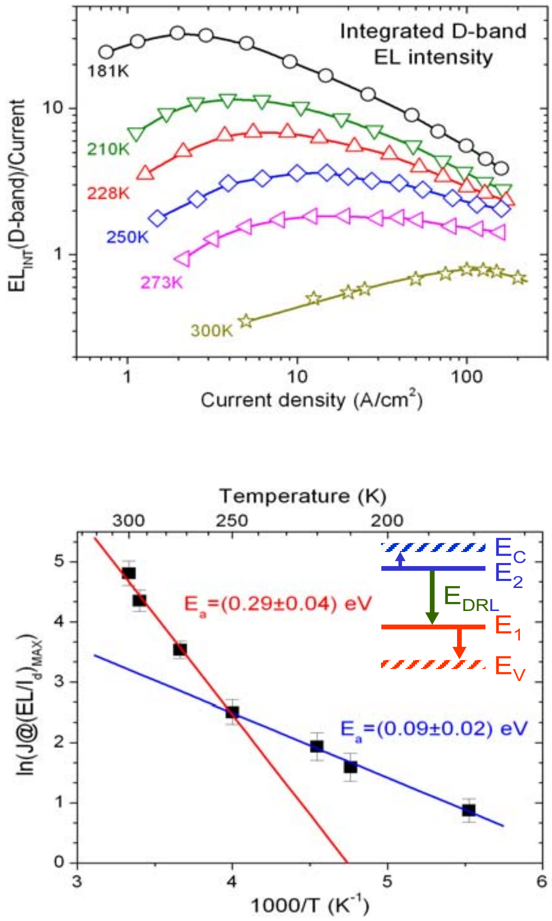

Figure 7 (a - top) Dependence of EL (i.e. electrically pumped DRL) at various temperatures normalized to the current from a diode containing dislocations. (b - bottom) Arrhenius plots of the specific current density values, i.e. the maxima in (a), fitted with two activation energies (shown in the figure). The inset in (b) shows the energy band diagram with radiative DRL and thermally stimulated carrier transitions.

3.3 Dislocation-based MOS-LED EL with BB emission at about 1.1 µm was reported from a MOS tunnel diode prepared on n-type Si [24]. Under positive gate bias electrons are attracted, building an accumulation layer close to the Si/oxide interface, and a hole current is formed by tunneling through the oxide layer. Also the MOS tunnel diodes on p-type Si yield comparable results. Fig. 8 shows the EL spectrum observed at room temperature exhibiting the BB peak with an efficiency > 0.1%. As shown in the inset the EL intensity increases sub-linearly with increasing tunneling current. The basic processes in MOS-LEDs on n-type and on p-type Si, respectively, are schematically represented in Fig. 9.

When a dislocation network with appropriate structure is positioned near the Si/oxide interface, close to/within the accumulation layer, the radiative recombination is dominated by the D1 peak at about 1.5 μm instead of the BB peak. This is clearly seen from the EL spectra shown in Fig. 10. More details about the mechanism originating the dislocation luminescence within the MOS-LED are described in [9b]. The MOS-LED on p-type Si, with the dislocation network at a depth of about 45 nm, consisted of a 134 nm thick Ti gate (7.9×10^{-3} cm^2) deposited on 1.8 nm thick Si oxide, see TEM micrographs shown in Fig. 11. The I-V characteristic is presented in the inset of Fig. 10. The tunneling current increases with increasing gate voltage, leading to an enhancement of the EL intensity. To estimate the efficiency, we compared the EL of a Si p-n diode under forward bias with that of the MOS-LED (Fig. 12), obtaining a value of about 0.1% for the 1.5 μm emission generated by the MOS-LED at 80 K. Increasing the temperature (T) from 80 to 210 K causes a reduction of the EL intensity/efficiency by a factor of about 2. Increase of temperature to 300 K was found to further reduce the EL efficiency.

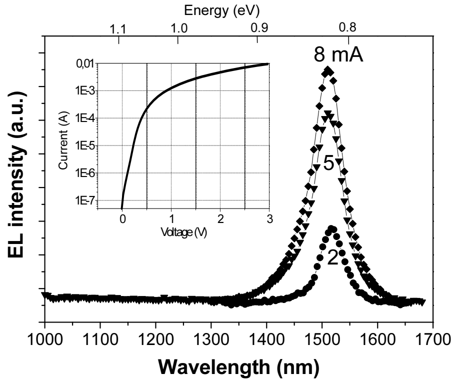

Figure 10 Electroluminescence at 80 K of a MOS-LED (gate area of about 7.9×10^{-3} cm^2) under negative gate bias with 1.5 μm radiation caused by the dislocation network near the Si/oxide interface. The intensity is found to increase sub-linearly with increasing tunneling current as seen from the spectra measured at 2, 5 and 8 mA, respectively. The inset represents the I-V characteristic of the LED at 300 K.

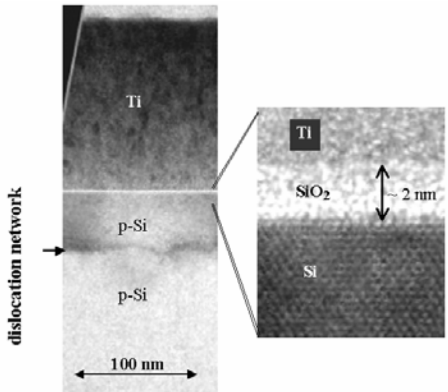

Figure 11 XTEM of the MOS-LED consisting of a 134 nm Ti layer on 1.8 nm Si oxide. The dislocation network is positioned in a depth of about 45 nm and was fabricated by direct bonding of p-type Si wafers, ρ ~ 10 Ωcm, with (100) orientation.

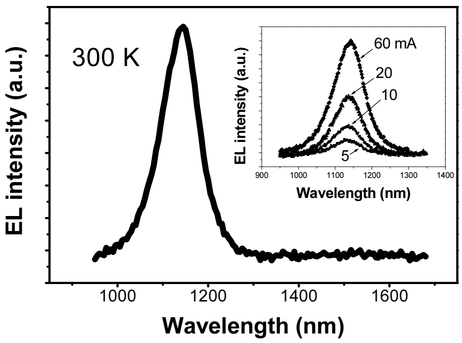

Figure 8 EL of a MOS tunnel diode on p-Si exhibiting BB luminescence at 300 K with an efficiency > 0.1 %. The inset shows the dependence of the EL signal on the current level.

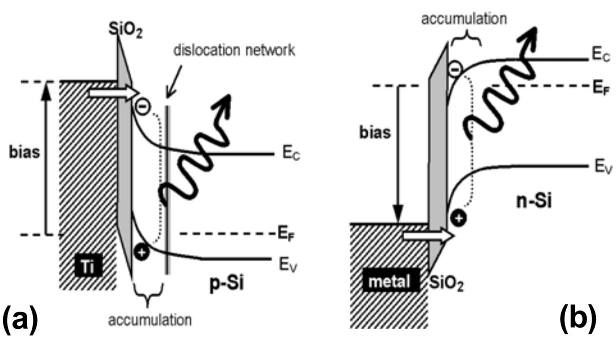

Figure 9 Scheme of MOS-LED, (a) p-type material with dislocation network, capable of yielding both dislocation and BB luminescence, (b) n-type Si without network yielding BB luminescence only.

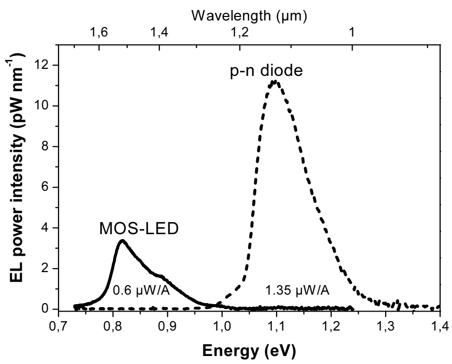

Figure 12 Comparison of the EL internal quantum efficiencies of a Si p-n diode and the MOS-LED. The p-n diode was measured at 300 K under forward bias, yielding an efficiency of 0.15%. For the MOS-LED, the estimated efficiency at 80 K was about 0.1%.

Nevertheless, we suppose that sufficient 1.5 µm luminescence at 300 K is achievable with dislocation networks, since clearly detectable D1 emission at 300 K (efficiency > 0.3%) was demonstrated already for a p-n LED containing a dislocation network, see below. Prospects for improvements of the MOS-LED are discussed in [9a].

3.4 Dislocation-based p-n LEDs Another way to get EL from the dislocation network is injection of excess carriers by a forward biased p-n junction, see Fig. 13a. A corresponding EL spectrum measured at room temperature is shown in Fig. 13b. The dislocation network was located in about 2 µm depth and produced by direct bonding of two p-type (100) Si wafers with 15 Ωcm resistivity. The p-n junction was formed by P implantation (energy 135 keV, 10^{14} ions per cm^2) and subsequent anneal. The internal efficiency at room temperature was measured at a forward current of 5 mA. It yields 0.95% for the BB line and 0.31% for the D1-line. This effect can be suppressed by using a mesa-like LED structure for carrier confinement

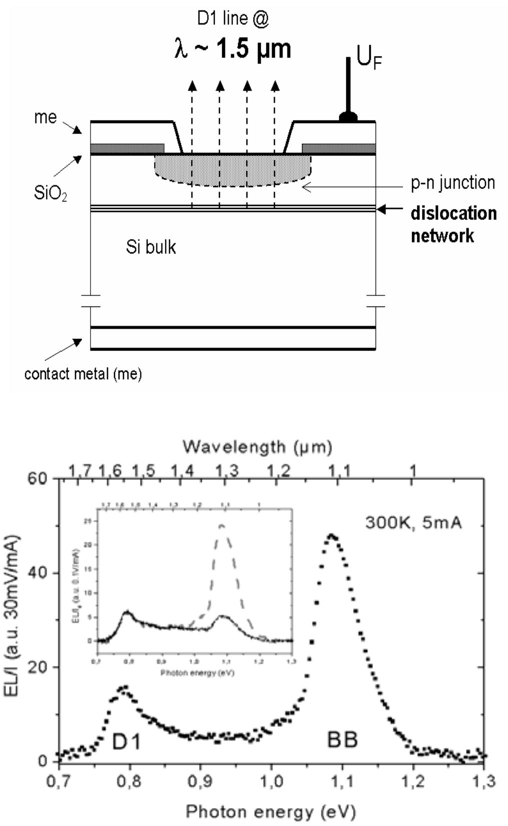

Figure 13 (a - top) Schematic view of a p-n LED based on D1 emission generated by a dislocation network in Si. (b - bottom) EL spectrum at 300 K for a 2 µm deep dislocation network yielding an efficiency > 0.3% for the D1-line at 1.55 µm and ~ 1% for the BB line. The inset shows the influence of the distance between p-n junction and dislocation network: network depth 0.26 µm for the full and 2 µm for the dashed line. Note, the appearance of the “background” luminescence in spectral range between D1 and BB lines is not yet fully understood.

The structure of the LED was mesa-like with an area of p-n junction and network of 0.1444 mm^2. It is important to note that the excess carriers are transported along the dislocation network (e.g. [25, 26]) which reduces their concentration and decreases the intensity/efficiency of light emission.. Moreover, the area of the mesa influences the efficiency. The depth of the dislocation network (distance between p-n junction and network) affects the spectrum and the ratio between D-band and BB-luminescence. This is shown in the inset of Fig. 13b, where the EL spectra of similar dislocation networks located in 2 µm or 0.26 µm depth, respectively, are compared. The spectra given in the inset were taken at room temperature for a forward current of 20 mA. Instead of dislocation networks also dislocation loops formed by implantation of Si ions and subsequent anneal can be used as D1-line light emitters [11], see below.

3.5 p-n LED with very high defect density In addition to the excitation condition, the sample temperature and the density of non-radiative recombination centers, the density of dislocations / extended crystal defects containing the levels forming the D1-line has a strong influence on the D1-intensity that can be reached. Use of microcrystalline Si in photovoltaics and microelectronics, which contains crystal defects in a very high density, provoked our interest to such material as a possible candidate for LED application. Investigation of pin structures produced by the CSG technology [http://www.csgsolar.com] show very promising results. EL spectra of such a junction at 300 K reveal the D1-line solely. Only at high carrier injection levels the D1 signal saturates and the BB line appears. The comparison of the EL signal from this device with a reference sample made from monocrystalline Si suggests that an internal efficiency up to 1% could be reached at 300 K (see Fig. 14).

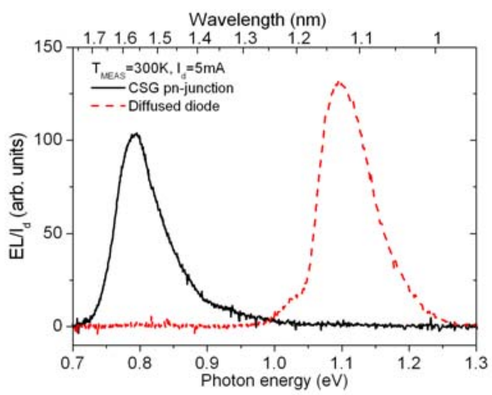

Figure 14 Comparison of the EL measured at 300 K of a p-n diode produced by diffusion in mono-crystalline Si that shows BB luminescence only and a pin diode fabricated according to the CSG technology. This diode contains a high density of crystal defects and exhibits D1 radiation only. Its efficiency is larger than that of the MOS-LED shown in Fig. 12 and of the p-n LED shown in Fig. 13.

Contributed Article

4 Stark effect for D-lines

4.1 Electro-luminescence from dislocation loops

Diodes formed by boron diffusion into n-type Si were implanted with 10^{15} Si^{+} ions per cm^2 with energies 200 and 450 keV and subsequently annealed at 950 °C for 20 min in nitrogen ambient to form dislocation loops (DL), see [11]. Figure 15 represents a scheme of the diode and a XTEM micrograph showing the DLs. The dislocation bands were located close to the p-n junction in the B doped p^{+}-layer and in the n-substrate, respectively. The EL spectrum of the diode exhibits the dislocation related peaks D1, D2 and D3, where D1 dominates, see Fig. 16. The spectral position of maximal intensity of D-band shifts to higher energy values with the increase in the carrier injection level (Fig. 17a). The blue shift for D-band was observed in a wide temperature (T) range between 30 K and 300 K. A thermal mechanism of this shift, related to the increased carrier injection, can be excluded because the heating should cause a red shift. Moreover, the position of the BB peak, which is also sensitive to T, did not change upon increase of the carrier injection level.

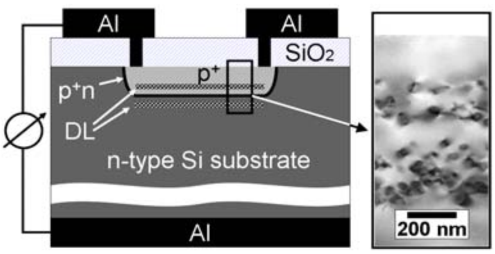

Figure 15 Schematic illustration of the cross-section of the p-n diode formed by B diffusion into n-type Si. Two bands of dislocation loops (DL) formed by Si implantation are shown in the XTEM micrograph.

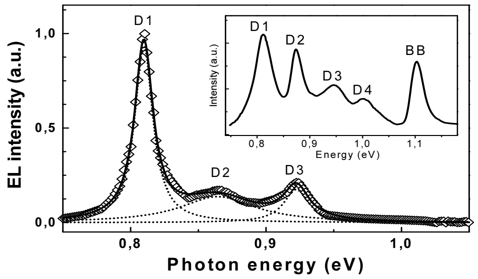

Figure 16 EL spectrum detected at 30 K from a LED containing dislocation loops. Decomposition of the spectrum shows three dislocation related lines D1-D3. For comparison, a typical luminescence spectrum of dislocated Si is given in the inset.

(a)

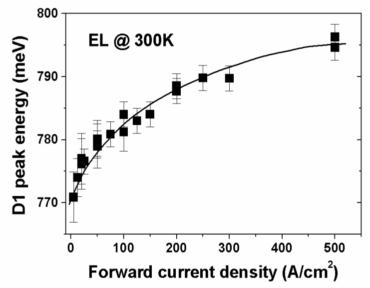

(b)

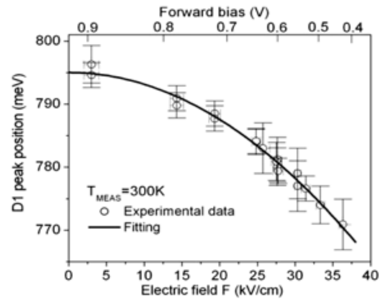

(c)

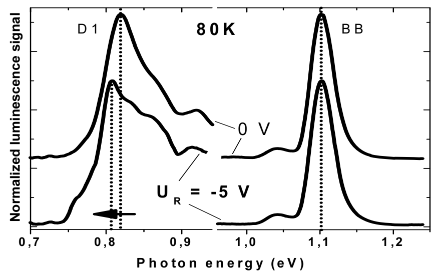

(d)

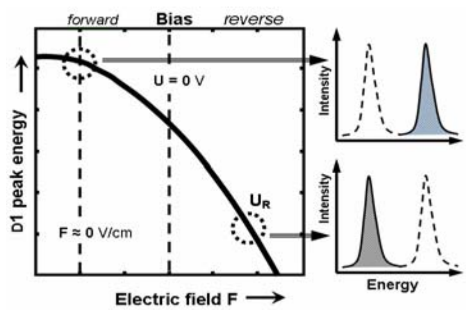

Figure 17 Influence of electric field on spectral position of the D1 line due to Stark effect. (a) Dependence of energy position of D1 peak on forward current density at 300 K. (b) Data from (a), shown as dependence of D1 position on electric field which was calculated from diode parameters and I-V characteristics. The data can be fitted by taking into account the quadratic Stark effect, see [26]. A red-shift of the D1 line is observed when increasing the field/reducing the forward bias. (c) Luminescence spectra of an optically pumped diode at 80 K for zero and reverse bias. A further red-shift of the D1 line is clearly visible when increasing the field/reverse bias. The spectra were normalized to the D1 and BB peak heights, respectively. (d) Schematic illustration of the shift of the spectral position of the D1 line caused by the electric field.

4.2 Stark effect at light emitting dislocations The dependence of the spectral position of the D1 peak on the *forward* current density observed in EL at 300 K is presented in Fig. 17a. An increase of the forward current corresponds to a reduction of the electric field (F) in the junction. In Fig. 17b the spectral position of the D1 peak is presented as a function of the electric field, exhibiting a red shift with increase of F.

The field was estimated from the junction parameters and the I-V curves. A *reverse* bias U_R applied to the p-n junction enhances the field F and led to a further growth of the red shift of the D1 peak, see Fig. 17c. For the measurements under the reverse bias, the excess carriers were pumped optically with 476 nm light. It should be stressed that the spectral position of the BB peak was not affected by the bias applied to the p-n junction (see Fig. 17c). The influence of the bias/electric field on the spectral position of the D1 light is sketched in Fig. 17d. The observed redshift of the D1 peak with increase in the field F can be understood in terms of the Stark effect, e.g. [27], which implies a quadratic shift in the excitonic transition energy E_{ex} caused by an electric field.

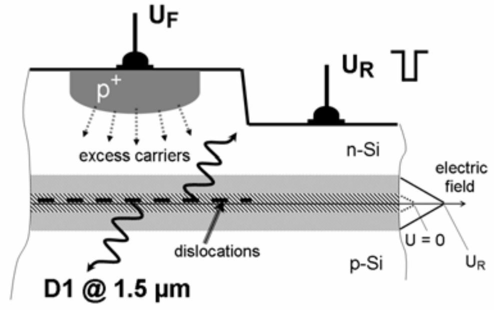

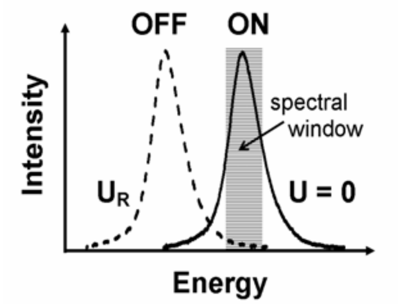

Figure 18 Combination of dislocation-based light emitter and electro-optical modulator within the same device. (a - top) Schematic drawing of the proposed device. Excess carriers are pumped by a forward biased p-n junction to cause the D1 peak emission. The electric field of the junction containing the dislocations is modulated with a reverse bias U_R. (b - bottom) Illustration of the light modulation due to the spectral shift of the D1 peak caused by the Stark effect. By applying a reverse bias U_R the emission is made to shift off the spectral window, leading to a modulation of the light intensity.

The relation $E_{ex} = E_{ex}(0) - \alpha F^2$, where $E_{ex}(0)$ is the energy of excitonic transition at F = 0 and α is a characteristic coefficient, describes the effect for $F \leq 50$ kV/cm. Fitting the experimental data presented in Fig. 17b yields $E_{ex}(0) = 795$ meV and $\alpha = 0.0186$ meV/(kV/cm)^2.

The Stark effect on dislocations, which appears to be considerably strong, was observed for the first time; for more details see [28]. It allows a controlled tuning of the spectral position of the D1 peak. If the spectral shift can be performed in a sufficiently short time, a combination of an electro-optical modulator with the light emitter can be realized. A fast modulation of the field F might be achieved with a reverse rather than with a forward bias.

4.3 Proposed novel modulator combined with the light emitter Figure 18 shows schematically the proposed device combining the dislocation-based light emitter and modulator. The excess carriers are pumped by a forward biased p-n junction to recombine radiatively at the dislocations. The modulation of the light is performed by switching the electrical field in the depletion region, which contains the dislocations, with a reverse bias. According to our estimates the light emitter offers the capability of > 1% efficiency at room temperature and the modulation should not remarkably reduce the light intensity. Dislocation networks could also be used instead of DLs in such devices. We believe that the Stark effect at dislocations in Si will allow realization of a novel electro-optical modulator which is fully compatible with Si technology. Its advantage is the combination of both - light emitter and modulator - within the same device.

Acknowledgements We would like to thank T. Hoang, J. Holleman and J. Schmitz (MESA+, University of Twente, The Netherlands) for fruitful discussions and the preparation of samples containing dislocation loops. Parts of this work were done within the framework of the SILEM project, funded by the German BMBF Ministry.

References

[1] H. Rong, A. Liu, R. Jones, O. Cohen, D. Hak, R. Nicolaescu, A. Fang, and M. Pannicia, Nature **433**, 292 (2005).
[2] L. Pavesi, J. Phys.: Condens. Matter **5**, R1169 (2003).
[3] W.L. Ng, M.A. Lourenco, R.M. Gwilliam, S. Ledain, G. Shao, and K.P. Homewood, Nature **410**, 192 (2001).
[4] J.M. Sun, T. Dekorsky, W. Skorupa, B. Schmidt, and M. Helm, Appl. Phys. Lett. **83**, 3885 (2003).
[5] N.A. Sobolev, A.M. Emel'yanov, E.I. Shek, and V.I. Vdovin, Solid State Phenomena **95/96**, 283 (2004).
[6] G.Z. Pan, R.P. Ostroumov, Y.G. Lian, K.N. Tu, and K.L. Wang, IEDM Tech. Digest (2004), pp. 343–346.
[7] M. Kittler, T. Arguirov, A. Fischer, and W. Seifert, Opt. Mater. **27**, 967 (2005).
[8] V. Kveder, M. Badylevich, E. Steinman, A. Izotov, M. Seibt, and W. Schröter, Appl. Phys. Lett. **84**, 2106 (2004).

[9a] M. Kittler, M. Reiche, X. Yu, T. Arguirov, O. F. Vyvenko, W. Seifert, T. Mchedlidze, G. Jia, and T. Wilhelm, IEDM Tech. Digest (2006), pp. 845–848.
[9b] X. Yu, W. Seifert, O.F. Vyvenko, M. Kittler, T. Wilhelm, and M. Reiche, Appl. Phys. Lett. **93**, 041108 (2008).
[10] M. Kittler, M. Reiche, T. Arguirov, W. Seifert, and X. Yu, IEDM Tech. Digest (2005), pp. 1027–1030.
[11] T. Hoang, J. Holleman, P. LeMinh, J. Schmitz, T. Mchedlidze, T. Arguirov, and M. Kittler, IEEE Trans. Electron Devices **54**, 1860 (2007).
[12] M.A. Green, J. Zhao, A. Wang, P. J. Reece, and M. Gal, Nature **412**, 805 (2001).
[13] A. Liu, R. Jones, L. Liao, D. Samara-Rubio, D. Rubin, O. Cohen, R. Nicolaescu, and M. Paniccia, Nature **427**, 615 (2004).
[14] Y.-H. Kuo, Y.K. Lee, Y. Ge, S. Ren, J.E. Roth, T.I. Kamins, D.A.B. Miller, and J.S. Harris, Nature **437**, 1334 (2005).
[15] D.K. Schroder, Solid State Phenomena **6/7**, 383 (1989).
[16] H. Schlangenotto, H. Maeder, and W. Gerlach, Phys. Status Solidi A **21**, 357 (1974).
[17] J. Dziewor and W. Schmid, Appl. Phys. Lett. **31**, 346 (1977).
[18] T. Trupke, J. Zhao, J. Zhao, A. Wang, R. Corkish, and M.A. Green, Appl. Phys. Lett. **82**, 2996 (2003).
[19] N.A. Drozdov, A.A. Patrin, and V.D. Tkachev, JETP Lett. **23**, 597 (1976).
[20] M. Reiche, K. Scheerschmidt, D. Conrad, R. Scholz, A. Plößl, U. Gösele, and K.N. Tu, Inst. Phys. Conf. Ser. **157**, 447 (1997).
[21] B. Aspar, M. Bruel, Moriceau, C. Maleville, T. Poumerol, A.M. Papon, A. Claverie et al., Microeletron. Eng. **36**, 233 (1997).
[22] X. Yu, O. Vyvenko, M. Kittler, W. Seifert, T. Mchedlidze, and T. Arguirov, M. Reiche, Semiconductors **41**, 458 (2007).
[23] V. Kveder, M. Badylevich, W. Schröter, M. Seibt, M. Steinman, and A. Izotov, Phys. Status Solidi A **202**, 901 (2005).
[24] C.W. Liu, M.H. Lee, M.-J. Chen, I.C. Lin, and C.-F. Lin, Appl. Phys. Lett. **76**, 1516 (2000).
[25] T. Mchedlidze, T. Wilhelm, X. Yu, T. Arguirov, G. Jia, M. Reiche, and M. Kittler, Solid State Phenomena **131–133**, 503 (2008).
[26] M. Kittler, X. Yu, T. Mchedlidze, T. Arguirov, O.F. Vyvenko, W. Seifert, M. Reiche, T. Wilhelm, M. Seibt, O. Voß, A. Wolff, and W. Fritzsche, Small **3**, 964 (2007).
[27] D.A.B. Miller, D.S. Chemla, T.C. Damen, A.C. Gossard, W. Wiegmann, T.H. Wood, and C.A. Burrus, Phys. Rev. B **32**, 1043 (1985).
[28] T. Mchedlidze, T. Arguirov, M. Kittler, T. Hoang, J. Holleman, J. Schmitz, Appl. Phys. Lett. **91**, 201113 (2007).

